ELSEVIER

Chemical Engineering Science 60 (2005) 4858–4865

Chemical Engineering Science

www.elsevier.com/locate/ces

Effect of surface free energy on the adhesion of biofouling and crystalline fouling

Q. Zhao[a,*], Y. Liu[a], C. Wang[a], S. Wang[b], H. Müller-Steinhagen[c]

[a]*Department of Mechanical Engineering, University of Dundee, Dundee DD1 4HN, UK*
[b]*School of Engineering, University of Surrey, Guildford GU2 7XH, UK*
[c]*Institute for Thermodynamics and Thermal Engineering, University of Stuttgart Institute for Technical Thermodynamics, German Aerospace Centre, D-7000 Stuttgart, Germany*

Received 29 January 2005; received in revised form 4 April 2005; accepted 4 April 2005
Available online 24 May 2005

Abstract

Pipelines and heat exchangers using seawater as coolant suffer from biofouling. Biofouling not only reduces heat transfer performance significantly, but also causes considerable pressure drop, calling for higher pumping requirements. It would be much more desirable if surfaces with an inherently lower stickability for biofouling could be developed. In this paper, a cost-effective autocatalytic graded Ni–Cu–P–PTFE composite coating with corrosion-resistant properties was applied to reduce biofouling formation. The experimental results showed that the surface free energy of the Ni–Cu–P–PTFE coatings, which were altered by changing the PTFE content in the coatings, had a significant influence on the adhesion of microbial and mineral deposits. The Ni–Cu–P–PTFE coatings with defined surface free energy reduced the adhesion of these deposits significantly. The anti-bacterial mechanism of the composite coatings was explained with the extended DLVO theory.

Keywords: Deposition; Coatings; Surface free energy; Adhesion; Biofouling; Corrosion

1. Introduction

The rapid development of the global offshore industry and of amphibious chemical, steel and power plants leads to more intensive use of seawater as a cooling medium. However pipelines and heat exchangers using seawater as coolant suffer from fouling, particularly biological fouling (Lucas et al., 1996; Koh et al., 1991). Biofouling of water-intake structures, equipment and power-plant piping is a major problem that affects condenser and heat exchanger availability and performance (Ritter and Suitor, 1975). Biofouling can lead to bio-corrosion of metal, which increases safety hazards from conventional and nuclear power plants (DiCinto and DeCarolis, 1993; Mussalli and Tsou, 1989). Because biofilms are highly hydrated, consisting of 98–99% water, their conductivity is similar to that of stationary water, but much lower than that of metals (Characklis, 1983). It therefore acts as an insulator, increasing heat transfer resistance, especially in heat exchangers. Very thin microfouling films can have a significant impact on the thermal performance of ocean thermal energy conversion (OTEC) heat exchangers (Kinelski, 1978). Biofouling not only reduces heat transfer performance significantly, but also causes considerable pressure drop, calling for higher pumping requirements. For example, biofouling on a 20-cm carbon steel pipe reduced the cross-sectional area by 52% in 2.5 years (Gaffoglio, 1987). The cost of cleaning and lost output can be extremely high.

Continuous chlorination of cooling water with concentration about 0.5–1.5 mg/l as Cl_2 has been the most widely used process to control biofouling (Allonier et al., 1999; Jenner et al., 1997; Rajagopal et al., 2003). Direct-cooled fossil

* Corresponding author. Tel.: +44 1382 345 651; fax: +44 1382 345 508.
E-mail address: q.zhao@dundee.ac.uk (Q. Zhao).

0009-2509/$ - see front matter © 2005 Elsevier Ltd. All rights reserved.
doi:10.1016/j.ces.2005.04.006

fuel and nuclear power stations on the coast typically use 30 and 45 m^3/s of seawater per 1000 MWe, respectively (Jenner et al., 1997). Therefore a large amount of chlorine is used everyday for disinfecting treatment and controlling biofouling. The generation and use of such large amounts of chlorine lead to pollution to the environment and the formation of halogenated by-products (Allonier et al., 1999). While trihalomethanes (THMs), which are suspected carcinogens, are the major compounds formed, other by-products are of concern due to their potential toxicity towards aquatic organisms. Any non-chemical method or less use of chemicals for inhibiting biofouling will reduce marine pollution significantly.

Since microbial adhesion on the surfaces of pipelines and heat exchangers in cooling water systems is a prerequisite for biofouling formation, prevention of microbial adhesion on the equipment surfaces will have a major impact in preventing biofouling. An effective and desirable approach to reduce cooling water biofouling is to alter the surface properties of the equipment and to make it less attractive for the fouling components, so that they can be removed easily from the surfaces by flowing water. The surface free energy of a solid surface gives a direct measure of intermolecular or interfacial attractive forces. Over the past two decades, marine bacterial adhesion to surfaces with different surface free energies has been investigated with the frequent conclusion that bacterial adhesion is less to low energy surfaces and easier to clean because of weaker binding at the interface (Dexter et al., 1975; Hamza et al., 1997). Dexter (Dexter et al., 1975) demonstrated low number of marine bacteria associated with low-energy substrates and high numbers on high-energy substrates. Milne and Callow (1985) also reported fewer bacteria adhering to a low surface energy material compared to a high surface energy material. Because of environmental restrictions on the use of biocides and organotin compounds, the Electric Power Research Institute (EPRI) sponsored tests evaluating 30 non-toxic coatings at eight sites in the coastal waters of the United States(Tsou and Mussalli, 1988). The test results indicated that silicon-based coatings performed satisfactorily. Although these coatings with low surface energy fouled, the fouling growth was easily removed from them. However, there are also a number of contrary findings, i.e., that hydrophilic surfaces (or high energy surfaces) have a lower biofouling tendency than hydrophobic surfaces (Brink et al., 1993; Fletcher and Marshall, 1982). Fattom and Shilo (1984) suggested that hydrophobic interactions play an important role in the initial adhesion process in some organisms. Baier et al. (1983) and Baier (1980) tried to minimize biological fouling of heat exchange surfaces by understanding, predicting and controlling the earliest events at the material/fluid interface. Baier (1980) also gave a relationship between surface free energy and relative bacterial adhesion. Fig. 1, known as the Baier curve, shows this relationship, and can partially explain the above inconsistent conclusion on the effects of surface free energy on bacterial adhesion. Clearly, there exists an optimum value of the surface free energy (about 25 mN/m) for which bacterial adhesion is minimal.

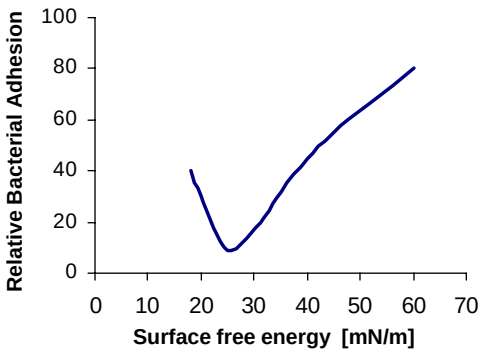

Fig. 1. Relative bacterial adhesion vs. surface free energy (Baier, 1980).

In addition to biofouling, crystalline fouling also occurs in heat exchangers using seawater as a coolant (Ritter and Suitor, 1975). Calcium carbonate, calcium sulphate or other salts that have solubility that diminishes with increasing temperature can form on exchanger tubes as crystalline deposits. Biofouling and crystalline fouling may occur singly or in combination depending on the operating parameters.

Many attempts have been made to reduce fouling by coating surfaces with PTFE due to its non-stick properties. However, the poor thermal conductivity, poor abrasion resistance and poor adhesion to metal substrate of the PTFE coatings currently inhibit their commercial use (Müller-Steinhagen and Zhao, 1997). The first electroless Ni–P–PTFE composite coatings were introduced about 24 years ago (Tulsi, 1983). The incorporation of PTFE nanoparticles into the Ni–P matrix can take advantage of the different properties of Ni–P alloy and PTFE. The resulting properties of electroless Ni–P–PTFE coatings, such as non-stick, higher dry lubricity, lower friction, good wear and good corrosion resistance, have been used successfully in many industries. Because the electroless Ni–P–PTFE coatings are metal-based, their thermal conductivity, anti-abrasive property, mechanical strength and adhesion strength to the substrate are superior to standard PTFE coatings. However, the corrosion resistance of the Ni–P–PTFE coatings needs to be improved, since the parts of the Ni–P–PTFE coatings were found to peel-off during long-term fouling tests with seawater due to corrosion. It was reported that the addition of copper into electroless Ni–P matrix could improve the corrosion resistance of the Ni–Cu–P coatings (Armyanov et al., 1999). In the paper, the Ni–Cu–P–PTFE composite coatings were developed and the corrosion rates of the Ni–Cu–P–PTFE composite coatings in NaCl solutions and the effects of surface free energy of Ni–Cu–P–PTFE coatings on the adhesion of microbial and $CaSO_4$ deposits were investigated.

2. Experimental procedure

2.1. Ni–Cu–P–PTFE composite coatings

To improve coating adhesion and corrosion resistance, a graded Ni–P/Ni–Cu–P/Ni–Cu–P–PTFE coating was coated on stainless steel 304 surfaces. The interlayer thickness of Ni–P/Ni–Cu–P was 2 μm. The Ni–Cu–P–PTFE composite coating was prepared by gradually increasing the PTFE content from the Ni–Cu–P interlayer to the top surface. Since there is no obvious interface between the coatings, the coating adhesion is improved significantly. The stainless steel samples were first cleaned with alkaline solution at 60–80 °C for 10–20 min and then rinsed with water. The compositions of the alkaline solution included 25 g/l NaOH; 25 g/l Na_2CO_3; 30 g/l Na_3PO_4 and 8 g/l Na_2SiO_3. The samples were dipped into a dilute HCl solution (1 M) for 30 s and then rinsed with cold water and deionized water, respectively. A 60% PTFE emulsion from Aldrich with a particle size in the range 0.05–0.5 μm was diluted with deionized water and stirred with a magnetic stirrer for 1 h. Then the solution was filtered with a filter of pore size 0.2 μm before use. The compositions of electroless Ni–Cu–P–PTFE solutions used in this investigation included 50 g/l $NiSO_4{\cdot}6H_2O$; 1.0 g/l $CuSO_4{\cdot}5H_2O$; 60 g/l $Na_3C_6H_5O_7{\cdot}2H_2O$; 25 g/l $NaH_2PO_2{\cdot}H_2O$; 40 g/l NH_4CH_3COO; 4–18 ml/l PTFE (60 wt%) and 0–0.6 g/l cationic surfactant. The coating thickness was measured using a digital micrometer and the coating compositions were analysed with an energy dispersive X-ray microanalysis (EDX) model JEOL T-300 at beam energy of 20 keV. The surface morphology of the coatings was analysed with a scanning electron microscope (SEM).

2.2. Corrosion rate measurement

The corrosion rates of the coatings in NaCl solutions were measured by a weight loss technique using a precise electric balance (resolution 10^{-5} g) and were compared with those of electroless Ni–P and Ni–P–PTFE, AISI 1020 low-carbon steel, stainless steel 304 and copper plates.

2.3. Contact angle measurements

Prior to contact angle measurement, samples were ultrasonically cleaned in acetone, ethanol and deionized water in sequence. Contact angles were obtained using the sessile drop method with a Dataphysics OCA-20 contact angle analyser. This instrument consists of a CCD video camera with a resolution of 768 × 576 pixel and up to 50 images per second, multiple dosing/micro-syringe units and a temperature controlled environmental chamber. The drop image was processed by an image analysis system, which calculated both the left- and right contact angles from the shape of the drop with an accuracy of ±0.1°. Three test liquids were used as a probe for surface free energy calculations: distilled water, diiodomethane (Sigma) and ethylene glycol (Sigma). The data for surface tension components of the test liquids are given in Table 1 (van Oss et al., 1988; Good, 1992). All measurements were made at 25 °C.

Table 1
Test liquids and their surface tension components (van Oss et al., 1988; Good, 1992)

Surface tension data (mN/m)	γ_L	γ_L^{LW}	γ_L^{AB}	γ_L^+	γ_L^-
Water (W), H_2O	72.8	21.8	51.0	25.5	25.5
Diiodomethane (D), CH_2I_2	50.8	50.8	0	0	0
Ethylene glycol (E), $C_2H_6O_2$	48.0	29.0	19.0	1.92	47.0

The contact angle of bacterial cells was measured on the lawns of bacteria deposited on membrane filters with pore diameter of 0.45 μm. Prior to contact angle measurement, the bacterial lawns were dried in air to a certain state, indicated by stable water contact angles. Usually this state of drying of a microbial lawn lasts 30–60 min and indicates that only bound water is present on the surface. The bacteria change their surface properties (such as surface energy) during their life-cycle. In this investigation, we investigated how surface energy of the coatings affects initial adhesion of bacteria. If initial bacterial adhesion strength is reduced by optimal surface free energy approach, they could be removed easily from the surfaces by flowing water. This may lead to a way of controlling biofouling formation. Therefore the surface energy of bacteria when they initially attach to the surface is required.

2.4. Surface free energy

The theory of the contact angle of pure liquids on a solid was developed nearly 200 years ago in terms of the Young equation (Young, 1805):

$$\gamma_L \cos\theta = \gamma_S - \gamma_{SL}, \tag{1}$$

where γ_L is the experimentally determined surface tension of the liquid, θ is the contact angle, γ_S is the surface free energy of the solid and γ_{SL} is the solid/liquid interfacial energy. In order to obtain the solid surface free energy γ_S an estimate of γ_{SL} has to be obtained. In 1962 Fowkes (Fowkes, 1964) pioneered a surface free energy component approach. He divided the total surface free energy into two parts: dispersive part and non-dispersive (or polar) part. The first part results from the molecular interaction due to London forces and the second part is due to all the non-London forces:

$$\gamma_i = \gamma_i^d + \gamma_i^p. \tag{2}$$

van Oss et al. (1988) developed an acid–base approach for the calculation of surface free energy. The surface free energy is seen as the sum of a Lifshitz–van der Waals apolar component γ_i^{LW} (corresponding to γ_i^d) and a Lewis acid–base

polar component γ_i^{AB} (corresponding to γ_i^p):

$$\gamma_i = \gamma_i^{LW} + \gamma_i^{AB}. \quad (3)$$

The acid–base polar component γ_i^{AB} can be further subdivided by using specific terms for an electron donor (γ_i^-) and an electron acceptor (γ_i^+) subcomponent:

$$\gamma_i^{AB} = 2\sqrt{\gamma_i^+ \gamma_i^-}. \quad (4)$$

The solid/liquid interfacial energy is then given by

$$\gamma_{SL} = \gamma_S + \gamma_L - 2\left(\sqrt{\gamma_S^{LW}\gamma_L^{LW}} + \sqrt{\gamma_S^+\gamma_L^-} + \sqrt{\gamma_S^-\gamma_L^+}\right). \quad (5)$$

Combining this with the Young equation (1), a relation between the measured contact angle and the solid and liquid surface free energy terms can be obtained:

$$\gamma_L(1+\cos\theta) = 2\left(\sqrt{\gamma_S^{LW}\gamma_L^{LW}} + \sqrt{\gamma_S^+\gamma_L^-} + \sqrt{\gamma_S^-\gamma_L^+}\right). \quad (6)$$

In order to determine the surface free energy components (γ_S^{LW}) and parameters γ_S^+ and γ_S^- of a solid, the contact angles of at least three liquids with known surface tension components (γ_L^{LW},γ_L^+, γ_L^-), two of which must be polar, have to be determined.

2.5. Bacterial adhesion

In this investigation, *Escherichia coli* (*E. coli*) *BL21* from Welcome Trust Bio-Center of University of Dundee was used for bacterial adhesion tests. A standard membrane filtration method was used to quantify the number of the bacterial colonies or colonies forming units (CFU) attaching to the treated and untreated surfaces (AWWA, 1998). After the frozen *E. coli BL21* was defrosted, it was cultured in Petri dishes with Luria–Bertani (LB) agar at 36.4 °C over night, and then colonized in 5 ml LB broth at 37 °C for 8 h. Finally, 5 ml *E. coli BL21* was diluted in 50 ml sterile deionized water. The coated and uncoated samples were exposed to the cell suspensions of *E. coli BL21* (about 1.9×10^9 cells/ml) on a shaker with 20–30 rpm. The contact times for these samples were 30 min at 22 °C, 5 h at 37 °C and 18 h at 37 °C. Then these samples were taken out and were put into 100 ml sterile deionized water under the stir conditions in order to remove the adhered bacteria into the water thoroughly. Then the water passed through membrane filters with a pore size 0.45 μm and *E. coli* remained on the filter surfaces. When the filters were replaced on growth medium-membrane lauryl sulphate broth (MLSB) in Petri dishes, the bacteria formed a small visible colony after 24 h incubation at 44 °C. The incubation at 44°C is to promote growth of *E. coli* and inhibit growth of other non-thermotolerant bacteria. The amount of *E. coli* on the filters was counted. If the water contains a large amount of bacteria, it needs to be diluted several times with a Ringer solution in order to count easily. Finally, the number of *E. coli* colonies (CFU/cm^2) on the surfaces was calculated.

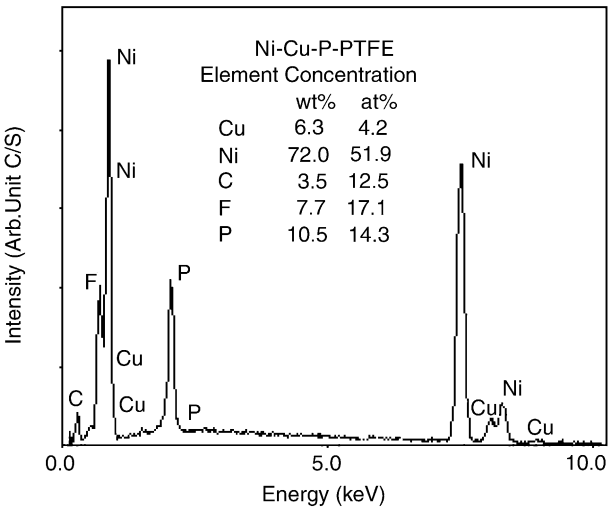

Fig. 2. EDX energy and elemental composition for a Ni–Cu–P–PTFE coating.

2.6. $CaSO_4$ deposit formation

Crystalline fouling tests were carried out in a pool boiling test rig at atmospheric pressure, which was described elsewhere (Müller-Steinhagen and Zhao, 1997). The rig contained 1.2 g/l $CaSO_4$ solution. The heaters were coated with the graded Ni–P/Ni–Cu–P/Ni–Cu–P–PTFE coatings with various surface energies. An untreated stainless steel heater was used as control. The heat flux of the heater was 100 kW/m^2. The $CaSO_4$ deposits which formed on each heater rod for a given heating time were removed. The deposit was dried and weighted using a Sartorius electronic scale with 10^{-5} g precision. Then the weight of the deposit per centimetre square heater surface was calculated.

3. Experimental results

3.1. Coating thickness, morphology and compositions

The thickness of the graded Ni–Cu–P–PTFE composite coatings was about 22 μm, including 2 μm Ni–P/Ni–Cu–P interlayer. The surface morphology of the coatings was analysed with a SEM, which confirmed that the PTFE particles were uniformly distributed throughout the Ni–Cu–P matrix. The compositions of the Ni–Cu–P–PTFE composite coatings were analysed with an energy dispersive X-ray microanalysis. Fig. 2 shows typical element compositions of the electroless Ni–Cu–P–PTFE composite coatings. The PTFE content was calculated based on F element content in the coating.

3.2. Corrosion rate measurement

Fig. 3 shows the comparisons of corrosion rates of the AISI 1020 low-carbon steel, copper, stainless steel 304,

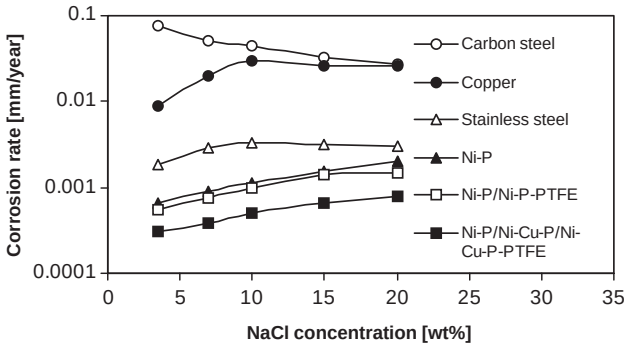

Fig. 3. Comparison of NaCl corrosion for graded Ni–Cu–P–PTFE, carbon steel, copper, stainless steel, Ni–P and Ni–P–PTFE.

Ni–P, graded Ni–P/Ni–P–PTFE and graded Ni–P/Ni–Cu–P/Ni–Cu–P–PTFE in NaCl solutions with the concentrations of 3.5, 7, 10, 15 and 20 wt%, respectively. The corrosion rates of the copper, stainless steel, Ni–P, Ni–P/Ni–P–PTFE or Ni–P/Ni–Cu–P/Ni–Cu–P–PTFE composite coatings increased with increasing NaCl concentration; while the corrosion rate of carbon steel decreased with increasing NaCl concentration. Steel corrodes in water according to the following reaction if oxygen exists:

$$\mathrm{Fe} = \mathrm{Fe}^{2+} + 2\mathrm{e}, \tag{7}$$

$$\tfrac{1}{2}\mathrm{O}_2 + \mathrm{H}_2\mathrm{O} + 2\mathrm{e} = 2\mathrm{OH}^-. \tag{8}$$

Overall reaction:

$$\mathrm{Fe} + \tfrac{1}{2}\mathrm{O}_2 + \mathrm{H}_2\mathrm{O} = \mathrm{Fe(OH)}_2. \tag{9}$$

The ferrous hydroxide is further oxidized to form rust by the reaction:

$$2\mathrm{Fe(OH)}_2 + \tfrac{1}{2}\mathrm{H}_2\mathrm{O} + \tfrac{1}{4}\mathrm{O}_2 = \mathrm{Fe(OH)}_3. \tag{10}$$

One may expect that the corrosion rate should increase with chloride content. This does indeed occur up to about 3 wt% NaCl (seawater concentration), but at high concentrations the rate decreases to values considerably less than for chloride-free water containing oxygen (Uhlig, 1971). The decrease results from a significant decrease in oxygen solubility with increasing chloride content (Uhlig, 1971). The corrosion rate of the Ni–Cu–P–PTFE coating was much lower than those of AISI 1020 low-carbon steel, copper, stainless steel 304, Ni–P coating and Ni–P–PTFE coating. The incorporation of copper into Ni–P–PTFE matrix improved the corrosion-resistant properties of the coatings. It was also reported that the addition of copper into electroless Ni–P matrix could improve the corrosion resistance of the Ni–Cu–P coatings (Armyanov et al., 1999).

3.3. Surface free energies of Ni–Cu–P–PTFE coatings and *E. coli BL21*

Fig. 4 shows the effects of PTFE content in the Ni–Cu–P–PTFE coatings on the surface free energy of the coatings. As the acid–base component (γ_S^{AB}) of the coatings is zero, the total surface free energy (γ_S) is equal to the dispersive component (γ_S^{LW}) of the coatings. Fig. 4 shows that the higher the PTFE proportion in the Ni–Cu–P–PTFE coatings, the lower the γ_S (or γ_S^{LW}) value of the coatings. The γ_S (or γ_S^{W}) value of stainless steel 304 is about 40 mN/m, which is much higher than that of the Ni–Cu–P–PTFE coatings. The surface free energy components (γ_1^{LW},γ_1^{+}, γ_1^{-}) of *E. coli BL21* were 35.40, 0.16 and 68.72 mN/m, respectively.

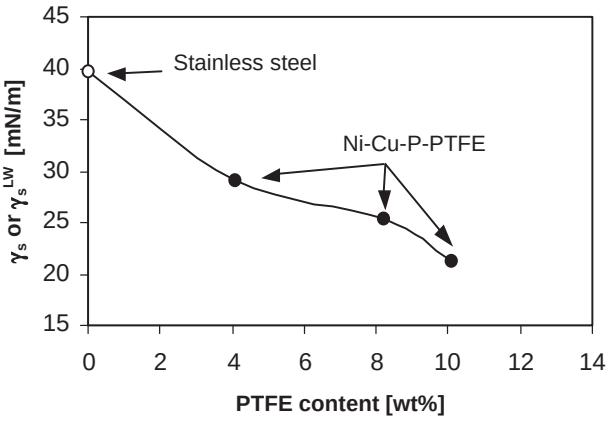

Fig. 4. Effect of the PTFE content in the Ni–Cu–P–PTFE coatings on the γ_S (or γ_S^{LW}) value of the coatings.

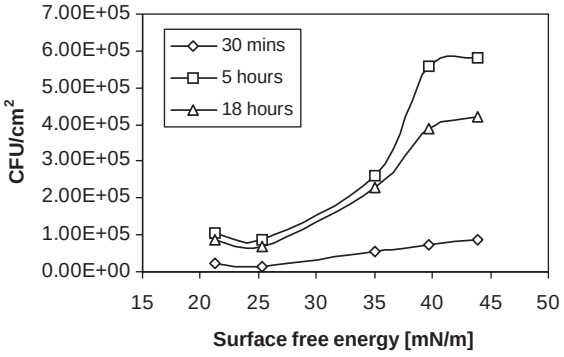

Fig. 5. Effect of surface free energy on *E. coli BL21* attachment at various contact time.

3.4. Bacterial adhesion

Fig. 5 shows the comparison of the numbers of cell colonies attached to a Ni–Cu–P–PTFE coated surface (PTFE 10.1 wt%; γ_S = 21.19 mN/m), a Ni–Cu–P–PTFE coated surface (PTFE 8.2 wt%; γ_S = 25.3 mN/m), a Ni–P coated surface (γ_S = 34.97 mN/m), a stainless steel 304 sheet (γ_S = 39.62 mN/m) and a titanium sheet (γ_S = 43.89 mN/m) at various contact times. The numbers of cell colonies attached to the surfaces decreased with decreasing surface energy and reached minimum when the surface energy of the coatings was about 26 mN/m, which was consistent with Baier' results (Baier, 1980). The Ni–Cu–P–PTFE coated

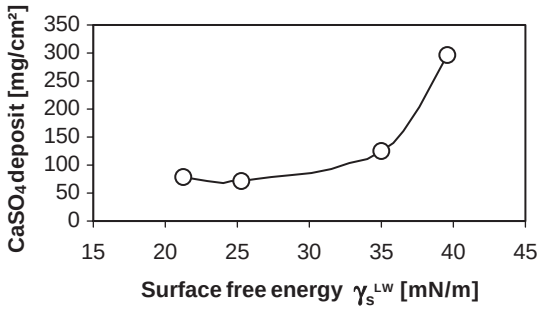

Fig. 6. Effect of the surface free energy on $CaSO_4$ formation.

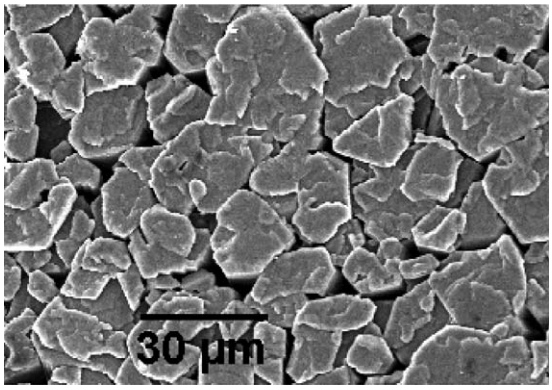

Fig. 7. $CaSO_4$ deposit formed on stainless steel surface.

surfaces performed best in inhibiting *E. coli* attachment, compared with stainless steel 304, titanium or Ni–P coating.

3.5. $CaSO_4$ fouling

Fig. 6 shows the comparison of the adhesion of $CaSO_4$ deposits on a Ni–Cu–P–PTFE coated surface (PTFE 10.1 wt%; $\gamma_S = 21.19$ mN/m), a Ni–Cu–P–PTFE coated surface (PTFE 8.2 wt%; $\gamma_S = 25.3$ mN/m), a Ni–P coated surface ($\gamma_S = 34.97$ mN/m) and a stainless steel 304 surface ($\gamma_S = 39.62$ mN/m). The surface free energy of the coatings has a significant influence on the adhesion of $CaSO_4$ deposits. When the surface free energy of the coatings was around 26–30 mN/m, the adhesion of $CaSO_4$ deposits was minimal.

Figs. 7 and 8 show the effect of surface free energy on the microstructure of $CaSO_4$ deposits. Fig. 7 shows that the deposit formed on the stainless steel surface with high surface free energy (39.62 mN/m) exhibits a packed structure. The density of the deposit on the surface was 2.9 g/cm^3. The deposit formed on the Ni–Cu–P–PTFE coated surface with low surface free energy (26 mN/m) exhibits a loose and porous structure with no defined orientation, as shown in Fig. 8. The density of the deposit on the coated surfaces was about 1.6 g/cm^3.

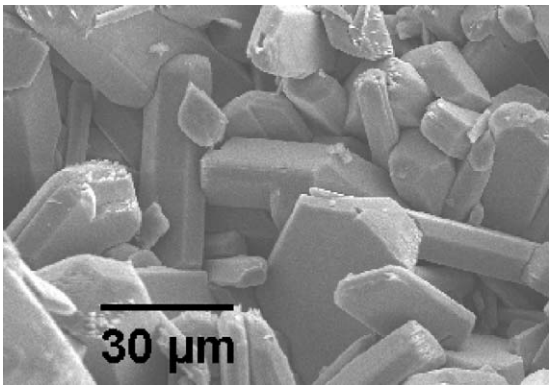

Fig. 8. $CaSO_4$ deposit formed on Ni–Cu–P–PTFE coated surface.

4. Discussion: adhesion mechanism

Bacterial adhesion may be described with the extended Deryagin, Landau, Verwey and Overbeek (DLVO) theory (Israelachvili, 1977; van Oss, 1994). According to the theory, the principal interaction forces determining hetero-coagulation include a Lifshitz–van der Waals (LW) interaction component, an electrostatic double-layer (EL) component, a Lewis acid–base (AB) component, and a Brownian motion (Br) (Israelachvili, 1977; van Oss, 1994). The total interaction energy $\Delta E_{132}^{\mathrm{TOT}}$ between bacteria 1 and a solid surface 2 in a fluid 3 can be written as the sum of these corresponding interaction terms (Israelachvili, 1977; van Oss, 1994; Oliveira, 1997):

$$\Delta E_{132}^{\mathrm{TOT}} = \Delta E_{132}^{LW} + \Delta E_{132}^{AB} + \Delta E_{132}^{EL} + \Delta E_{132}^{\mathrm{Br}}. \tag{11}$$

The balance between all possible interactions determines whether or not the bacteria will attach on the surface: adhesion will take place when $\Delta E_{132}^{\mathrm{TOT}}$ is negative (i.e., total interaction force is attractive) (Oliveira, 1997).

Recently, Zhao and Müller-Steinhagen (2002) derived the optimum surface free energy components of a surface, for which bacterial adhesion force is minimal, using the extended DLVO theory:

$$\sqrt{\gamma_S^{LW}} = (1/2)\left(\sqrt{\gamma_1^{LW}} + \sqrt{\gamma_3^{LW}}\right), \tag{12}$$

$$\gamma_S^- = \left(\frac{\sqrt{\gamma_1^-\gamma_S^+} + \sqrt{\gamma_3^+\gamma_3^-} - \sqrt{\gamma_3^-\gamma_S^+} - \sqrt{\gamma_1^+\gamma_1^-}}{\sqrt{\gamma_3^+} - \sqrt{\gamma_1^+}}\right)^2, \tag{13}$$

$$\gamma_S^{\mathrm{TOT}} = \gamma_S^{LW} + 2\sqrt{\gamma_S^+\gamma_S^-}, \tag{14}$$

where γ_S^{LW}, γ_1^{LW} and γ_3^{LW} are the LW surface free energy of the surface (e.g. coating), particles (e.g. bacteria) and fluid (e.g. water), respectively. They can be determined

experimentally. We found that the γ_S^+ values for the solid materials and coatings are near zero. If we assume $\gamma_S^+ = 0$, then the optimum surface energy of the solid surface can be calculated using the following very simple equation:

$$\gamma_S^{\mathrm{TOT}} = \gamma_S^{LW} = \frac{1}{4}\left(\sqrt{\gamma_1^{LW}} + \sqrt{\gamma_3^{LW}}\right)^2. \quad (15)$$

As the equation isolates the effect of surface free energy upon particulate adhesion from the numerous parameters in the extended DLVO theory, it appears relatively simple.

Eq. (15) explains the experimental results—why bacterial adhesion was minimal when the LW surface free energy of the coatings was about 25.3 mN/m. The γ_1^{LW} value of *E. coli BL21* was 35.4 mN/m and γ_3^{LW} of water was 21.8 mN/m. Eq. (15) then produces a theoretical value of $\gamma_S^{\mathrm{TOT}} = 28.18$ mN/m, which approximates the experimental value of the surface free energy for which *E. coli* attachment was minimal. According to Förster and Bohnet (2000), the average LW surface free energy of $CaSO_4$ deposits, γ_1^{LW} was around 37 mN/m, and the γ_3^{LW} of water is 21.8 mN/m. Eq. (15) then produces a surface free energy value $\gamma_S^{\mathrm{TOT}} = 29$ mN/m, which approximates the experimental value of the surface free energy (25–30 mN/m) for which the precipitation of $CaSO_4$ salt on heat transfer surfaces was minimal.

In addition to surface free energy, other factors, including surface charge, surface roughness, temperature, contact time and fluid flow velocity also have significant influence on bacterial adhesion or $CaSO_4$ adhesion (Ritter and Suitor, 1975; Karabelas, 2002). Therefore the mechanisms of bacterial adhesion or $CaSO_4$ adhesion are complex. If initial bacterial or $CaSO_4$ adhesion strength is reduced by an optimal surface free energy approach, they could be removed easily from the surfaces by flowing water. This may lead to a way of controlling biofouling or mineral fouling formation.

5. Conclusions

The surface free energy of the Ni–Cu–P–PTFE coated surfaces has a significant influence on the bacterial (or $CaSO_4$ deposit) adhesion. When the surface free energy of the Ni–Cu–P–PTFE coated surfaces was in the range 25–30 mN/m, the adhesion of both bacteria and $CaSO_4$ deposit was minimal. The graded electroless Ni–Cu–P–PTFE composite coatings with corrosion resistant properties have a potential for reducing biofouling and mineral fouling.

Acknowledgements

This work was supported by the Engineering and Physical Sciences Research Council, UK.

References

Allonier, A.S., Khalanski, M., Camel, V., Bermond, A., 1999. Characterization of chlorination by-products in cooling effluents of coastal nuclear power stations. Marine Pollution Bulletin 38, 1232–1241.

Armyanov, S., Georgieva, J., Tachev, D., Valova, E., Nyagolova, N., Mehta, S., Leibman, D., Ruffini, A., 1999. Electroless deposition of Ni-Cu-P alloys in acidic solutions. Electrochemical and Solid State letters 2, 323–325.

AWWA, 1998. Standard Methods for the Examination of Water and Wastewater, 20th ed. AWWA.

Baier, R.E., 1980. Adsorption of Micro-organisms to Surface. Wiley-Interscience Publishers, New York, pp. 59–104.

Baier, R.E., Meyer, A.E., DePalma, V.A., King, R.W., Fornalik, M.S., 1983. Surface microfouling during the induction period. Journal of Heat Transfer 105, 618–624.

Brink, L.E.S., Elbers, S.J.G., Robbertsen, T., Both, P., 1993. The anti-fouling action of polymers preadsorbed on ultrafiltration and microfiltration membranes. Journal of Membrane Science 76, 281–291.

Characklis, W.G., 1983. Process analysis in microbial systems: biofilms as a case study. In: Bazin, M. (Ed.), Mathematics in Microbiology. Academic Press, pp. 171–234.

Dexter, S.C., Sullivan, J.D., Williams, J., Watson, S.W., 1975. Influence of substrate wettability on the attachment of marine bacteria to various surfaces. Applied Microbiology 30, 298–308.

DiCinto, R.A., DeCarolis, G., 1993. Biofouling and corrosion. Corrosion Prevention & Control 40, 104–107.

Fattom, A., Shilo, M., 1984. Hydrophobicity as an adhesion mechanism of benthic cyanobacteria. Applied and Environmental Microbiology 47, 135–143.

Fletcher, M., Marshall, K.C., 1982. Are solid surfaces ecological significance to aquatic bacteria? Advances in Microbial Ecology 47, 135–143.

Förster, M., Bohnet, M., 2000. Modification of molecular interactions at the interface crystal/heat transfer surface to minimize heat exchanger fouling. International Journal of Thermal Sciences 39, 697–708.

Fowkes, F.M., 1964. Dispersion force contributions to surface and interfacial tensions, contact angles, and heats of immersion. Advances in Chemistry 43, 99–111.

Gaffoglio, C.J., 1987. Beating biofouling with copper–nickel alloys offshore. Sea Technology 28, 43–46.

Good, R.J., 1992. Contact-angle, wetting, and adhesion—A critical—review. Journal of Adhesion Science and Technology 6, 1269–1302.

Hamza, A., Pham, V.A., Matsuura, T., Santerre, J.P., 1997. Development of membranes with low surface energy to reduce the fouling in ultrafiltration applications. Journal of Membrane Science 131, 217–227.

Israelachvili, J.N., 1977. Intermolecular and Surface Forces. second ed. Academic Press, London.

Jenner, H.A., Taylor, C.J.L., vanDonk, M., Khalanski, M., 1997. Chlorination by-products in chlorinated cooling water of some European coastal power stations. Marine Environmental Research 43, 279–293.

Karabelas, A.J., 2002. Scale formation in tubular heat exchangers-research priorities. International Journal of Thermal Science 41, 682–692.

Kinelski, E.H., 1978. Proceedings of the Fifth Ocean Thermal Energy Conversation Conference, Miami Beach FL, pp. VIII. 1–VIII. 6.

Koh, L.L., Hong, W.K., Lip, L.K., 1991. Ecology of marine fouling organisms at eastern Johore strait. Environmental Monitoring and Assessment 19, 319–333.

Lucas, K.E., Bergh, J.O., Christian, D.K., 1996. Dechlorination equipment development for shipboard pollution prevention. Naval Engineers Journal 108, 19–25.

Milne, A., Callow, M.E., 1985. Non-biocidal anti-fouling processes. In: Smith, R. (Ed.), Polymers in Marine Environment. The Institute of Marine Engineers, London, pp. 229–233.

Müller-Steinhagen, H., Zhao, Q., 1997. Investigation of low fouling surface alloys made by ion implantation technology. Chemical Engineering Science 52, 3321–3332.

Mussalli, Y.G., Tsou, J., 1989. Proceedings of the 51st American Power Conference, pp. 1094–1099.

Oliveira, R., 1997. Understanding adhesion: a means for preventing fouling. Experimental Thermal and Fluid Science 14, 316–322.

Rajagopal, S., Venugopalan, V.P., Van der Velde, G., Jenner, H.A., 2003. Comparative chlorine and temperature tolerance of the oyster *Crassostrea madrasensis*: implications for cooling system fouling. Biofouling 19, 115–124.

Ritter, R.B., Suitor, J.M., 1975. Handling and disposal of solid. Proceedings of the Second NATL Conference on Complete Water Reuse. Water's Interface with Energy, Air and Solids, Chicago, IL, 604–609.

Tsou, J., Mussalli, Y.G., 1988. Advances in nontoxic biofouling control technologies. American Society of Mechanical Engineers, Heat Transfer Division, vol. 1, pp. 231–237.

Tulsi, S.S., 1983. Composite PTFE–nickel coatings for low friction applications. Finishing 7, 14–18.

Uhlig, H.H., 1971. Corrosion & Corrosion Control, second ed. Wiley, New York, p. 113.

van Oss, C.J., 1994. Interfacial Forces in Aqueous Media. Marcel Dekker, New York.

van Oss, C.J., Good, R.J., Chaundhury, M.K., 1988. Additive and nonadditive surface-tension components and the interpretation of contact angles. Langmuir 4, 884–891.

Young, T., 1805. An essay on the cohesion of fluids. Philosophical Transactions of the Royal Society London 95, 65–87.

Zhao, Q., Müller-Steinhagen, H., 2002. Intermolecular and adhesion forces of deposits on modified heat transfer surfaces. In: Müller-Steinhagen, H. et al. (Eds.), Heat exchanger fouling—Fundamental Approaches and Technical Solutions. Publico Publ, Essen, pp. 41–46.